Evaluation of Transducers with Near-field Scanning of Their Surfaces

Jian-yu Lu and James F. Greenleaf

Biodynamics Research Unit, Department of Physiology and Biophysics,
Mayo Clinic and Foundation, Rochester, MN 55905 U.S.A.

Abstract—Recently, near-field imaging has been studied in microwaves, optics, and acoustics. In this paper, we study the near-field imaging of wave sources and thus the structure of transducers in high resolution. In addition, we report the near-field imaging of array transducers that were driven with alternating phases on adjacent elements. This produces high contrast images of the array structures. Results suggest that these methods may be useful for transducer manufacturers, designers, and researchers.

I. INTRODUCTION

Near-field imaging is a technique that probes the local property of an object using information carried by waves before they diffract significantly. Near-field imaging can achieve spatial resolution that is higher than the limit imposed by wavelength in regular imaging. Theoretically, the spatial resolution of the near-field imaging is limited only by the size of tip (probe) that interacts with the object to be imaged (super resolution). Near-field imaging was first demonstrated in microwave [1] and then applied to optics [2] and acoustics [3] and has been studied by many other investigators [4–12].

In this paper, we report near-field imaging of wave sources to study structures of transducers in high resolution with a 0.5 mm diameter hydrophone scanning very close to the surfaces of the transducers. In addition, we have developed a method that is effective for imaging the surfaces of either annular or linear arrays. This method applies alternating phases (difference by 180°) to drive adjacent array elements and obtains the structures (related to the acoustic pressures produced) of arrays by near-field imaging. Because the alternating phases produce zero pressure between elements, the contrast of the images of the arrays is increased. This method may be useful for quality control in array production. In the following, we will demonstrate experimentally the efficacy of the methods developed.

II. EXPERIMENT METHOD

Fig. 1 is the block diagram of the experiment. One-and-a-half cycle short pulses (produced by the Polynomial Waveform Synthesizer, Model DATA 2045) were amplified (with an ENI rf power amplifier, Model 240L) to drive the transducers. At a constant distance from the surface of the transducers, a 0.5 mm diameter hydrophone was used to scan the transducer surfaces in a raster format (C-Scan). Signals received were digitized and stored in a MC68000 computer for further processing. Because most of transducers work in the half wavelength resonance mode, the first and second half cycles of the vibration are related closely to the structures of the front and the back surfaces of the transducers, respectively. Therefore, we have rectified and averaged the first and the second half cycles of the pressure signals to represent the front and back surfaces of the transducers, respectively (see lower part of Fig. 1). The average process reduces the noise caused by the vibration of the scanner.

III. RESULTS

Unfocused air-backed piston transducers of 1.5 MHz and 2.0 MHz central frequencies were scanned near their front surfaces to show both the front surfaces and the wire connections on the back surfaces (Fig. 3). In addition, a 0.75 MHz central frequency (wavelength, λ, was 2 mm in water) ceramic transducer was cut with a diamond saw to form two resolution patterns perpendicular to each other (Fig. 2). The transducer was air backed and scanned by the hydrophone near its front surface. Images that represent the front and back surfaces were obtained. The

1051-0117/94/0000-1163 $4.00

image that has the highest spatial resolution is that of the front surface scanned at the distance of 0.05λ. The resolution is about 0.5 mm, much smaller than the wavelength and is close to the diameter of the hydrophone (Fig. 4).

Both annular and linear array transducers were studied. They were driven by alternating phases between adjacent elements and imaged in near field that revealed clearly the array structures (Figs. 5 and 6). Images obtained with in-phase drive are also shown for comparison.

IV. DISCUSSION

The near-field scanning of transducers can achieve super-resolution imaging of the active structures of transducers (Fig. 3). However, there are limitations. The distance between hydrophone and the surface of transducer must be very small. Only the surface that is scanned has the highest resolution. To obtain high resolution on the other surface, the transducers can be flipped over and scanned or they must be very thin (have high central frequency). With our current scanner system, only transducers with flat surfaces can be studied. Curved transducers must be scanned with a more complex system that has servo control to keep the distance between the transducer and hydrophone constant. In addition, the distance between transducers and hydrophone is limited by front matching layers or lenses. To increase the resolution of this method, the size of the hydrophone must be very small. But small hydrophones have increased impedance and thus lower signal-to-noise ratio.

Near-field imaging of array transducers that are driven by alternating phases on adjacent elements has both high resolution and high contrast. The zeroes between elements help to distinguish the elements clearly even if their sizes are smaller than a wavelength (Fig. 6). In contrast, the array elements are hard to see in the images obtained with in-phase drive (Fig. 6).

V. CONCLUSION

Near-field scanning of transducer surfaces with a hydrophone is a useful method to study transducers in high resolution. Driving transducer elements with alternating phases may even enhance the method. These methods are potentially useful for transducer manufacturers, designers, and researchers.

VI. ACKNOWLEDGMENTS

The authors appreciate the secretarial assistance of Ms. Elaine C. Quarve. The authors also thank Echo Ultrasound[1] for cutting the resolution patterns on the 0.75 MHz transducer. This work was supported in part by grants CA 43920 and CA 54212 from the National Institutes of Health.

VII. REFERENCES

1. E. A. Ash and G. Nicholls, "Superresolution aperture scanning microscope," *Nature*, vol. 237, p. 510, June 30 1972.
2. E. Betzig, J. K. Trautman, T. D. Harris, J. S. Weiner, and R. L. Kostelak, "Breaking the Diffraction Barrier: optical microscopy on a nanometric scale," *Science*, vol. 251, p. 1468, 1991.
3. B. T. Khuri-Yakub, C. Cinbis, C. H. Chou, and P. A. Reinholdtsen, "Near-field scanning acoustic microscope," *IEEE 1989 Ultrasonics Symposium Proceedings* 89CH22791-2, vol. 2, pp. 805-807, 1989.
4. W. Durr, D. A. Sinclair, and E. A. Ash, "A high resolution acoustic probe," *Electronic Letters*, vol. 21, p. 805, 1980.
5. J. K. Zienuk and A. Latuszek, "Ultrasonic pin scanning microscope — a new approach to ultrasonic microscopy," *IEEE 1986 Ultrasonics Symposium Proceedings*, 86CH2375-4, vol. 2, pp. 1037-1039, 1986.
6. K. Takata, T. Hasegawa, S. Hosaka, S. Hosoki, and T. Komoda, "Tunneling acoustic microscope," *Applied Physics Letters*, vol. 55. p. 1718, 1989.
7. P. Gunther, U. Ch. Fisher, and K. Dransfeld, "Scanning nearfield acoustic microscopy," *Applied Physics B*, vol. 48, p. 89, 1989.
8. J. K. Zieniuk and A. Latuszek, "Non-conventional pin scanning ultrasonic mi-

[1] Echo Ultrasound Inc., Lewistown, PA

croscopy," *Acoustical Imaging*. New York, Plenum Press, 1989, vol. 17, pp. 219–224.
9. B. T. Khuri-Yakub, S. Akamine, B. Hadimioglu, H. Yamada and C. F. Quate, "Near field acoustic microscopy," *SPIE Scanning Microscopy Instrumentation*, vol. 1556, p. 30, 1991.
10. A. Kulik, J. Attal, and G. Gremaud, "Nearfield scanning microscopy," *Acoustical Imaging*. New York, Plenum Press, 1993, vol. 20, pp. 331–343.
11. U. Ch. Fischer, "Optical characteristics of 0.1 μm circular apertures in a metal film as light sources for scanning ultramicroscopy," *Journal of Vacuum Science and Technology B*, vol. 3, no. 1, p. 386, January/February 1985.
12. E. Betzig, A. Lewis, A. Harootunian, M. Isaacson, and E. Kratschmer, "Near-field scanning optical microscopy (NSOM)," *Biophysics Journal*, vol. 49, p. 269, January 1986.

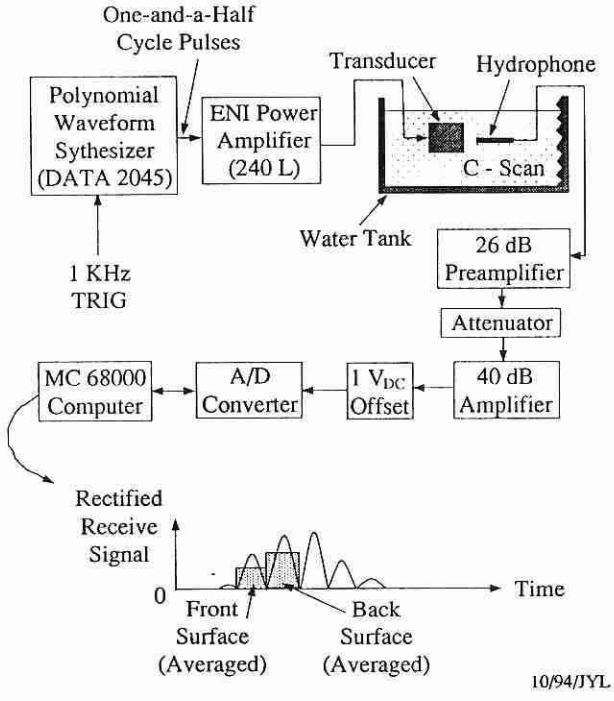

Fig. 1 Block diagram of near-field scan of transducer surfaces. One-and-a-half cycle pulses were amplified to drive transducers that were immersed in a water tank. The acoustic pressure produced was measured point-by-point with a 0.5 mm diameter hydrophone scanning in a raster format (C-scan) at a constant distance. The received signals were amplified, digitized and stored in a computer. The whole system was synchronized with a 1 KHz trigger signal. A rectified sample waveform is shown in the lower part of the figure. The first and the second half cycles of the signals were averaged to represent the front and the back surfaces of the transducers, respectively.

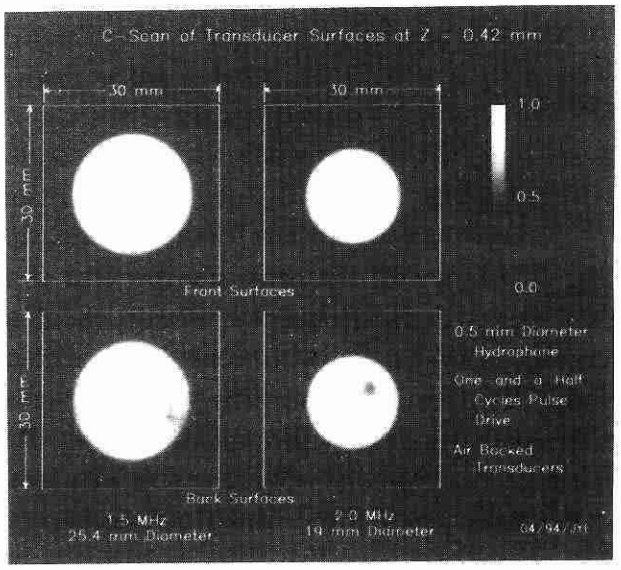

Fig. 2 Images of 1.5 MHz and 2.0 MHz central frequency air-backed transducers obtained at distances of 0.42λ and 0.56λ, respectively (λ is wavelength in water). Their diameters were 25.4 and 19 mm, respectively. The upper and lower two panels are images of acoustic pressures that were obtained by processing the received signals as described in Fig. 1 to represent the front and the back surfaces of the transducers. In the images of the back surfaces, the wire connections to the electrodes of the transducer elements are clearly seen.

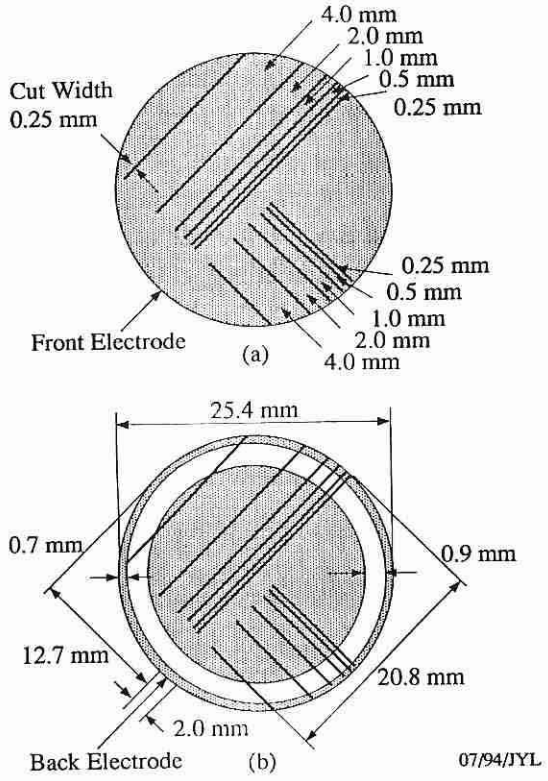

Fig. 3 Diagram of the resolution patterns of a 0.75 MHz central frequency transducer. The transducer was coated with front and back electrodes. Two resolution patterns perpendicular to each other were cut with a diamond saw. The cuts extended from the front to the back surfaces of the transducer and the width of the cuts was 0.25 mm. There were five different spacings between the cuts: 4.0, 2.0, 1.0, 0.5, and 0.25 mm, respectively. The diameter of the transducer is 25.4 mm.

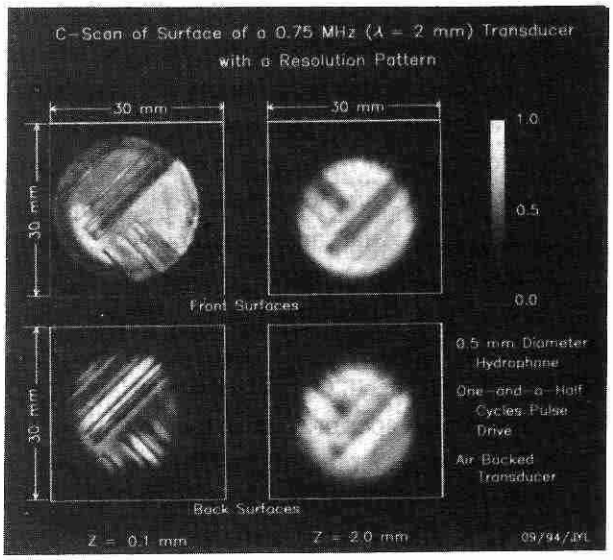

Fig. 4 Images of the 0.75 MHz central frequency (wavelength λ = 2 mm in water) air-backed transducer with the resolution patterns shown in Fig. 3. They were obtained at two scanning distances: 0.05λ (left two panels) and 1.0λ (right two panels). The upper and lower two panels are images of acoustic pressures obtained by processing the received signals as described in Fig. 1 to represent the front and the back surface of the transducer. At the distance of 0.05λ, the image of the front surface shows clearly the resolution patterns with a resolution of about 0.5 mm. The resolution patterns of the back surface were distorted because their distance to the hydrophone was larger. Both the images of the front and back surfaces obtained at the distance of 1.0λ were blurred.

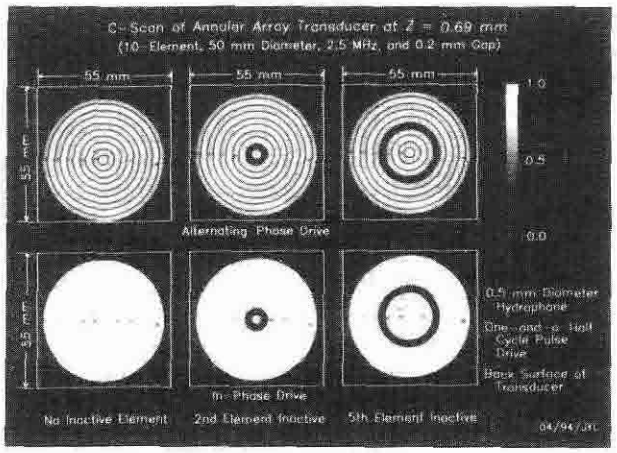

Fig. 5 Near-field images of the back surface of a 10–element, 2.5 MHz central frequency (wavelength λ = 0.6 mm), and 50 mm diameter annular array transducer obtained at the distance of 1.15λ. The transducer was made of 1–3 PZT ceramics/polymer composite materials. It had a flat front electrode (ground) and 10 concentric annular back electrodes. The gap between the electrodes was about 0.2 mm and the width of the electrodes was about 2 mm. The upper panels are results with the transducer driven by alternating phases, and the lower are those with the transducer driven by the same phases for all elements. From left to right, the panels show images with all elements active, with the second, and with the fifth element disconnected. It is seen that with alternating phase drive, the structure of the array is more clearly shown as compared to those with the in-phase drive. The wire connections of the back electrodes are seen in both alternating phase and in-phase drive images.

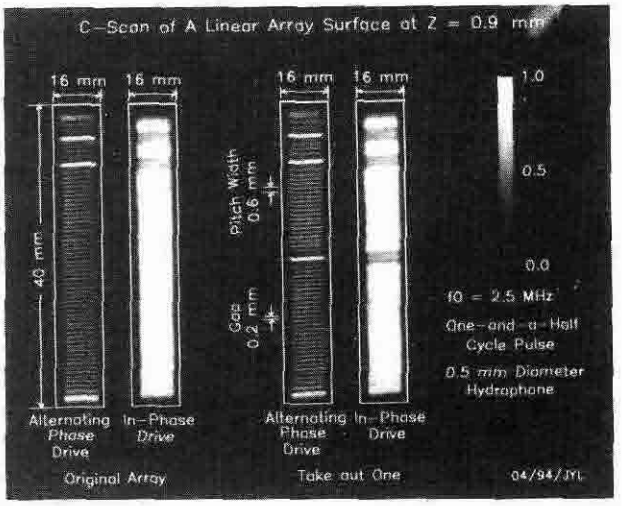

Fig. 6 Near-field images of the front surface of a 64–element, 2.5 MHz central frequency (wavelength λ = 0.6 mm) linear array transducer obtained at the distance of 1.5λ. The transducer was made of PZT ceramics cut into strips. The dimension of the ceramic was 38.4 mm (long) and 10 mm (wide). The array had a flat front electrode (ground) and 64 back electrodes. The gap between the elements was about 0.2 mm and the distance between the centers of the elements was about 0.6 mm. There are two groups of images from left (without taken out any elements) to right (taken out the 33rd element). Each group consists of two panels. The left one in each group was obtained by driving the array in alternating phases, and the right was obtained by driving all elements in phase. It is seen that with alternating phase drive, every element is clearly visible as compared to those with the in-phase drive where no element is distinguishable. Two elements that were originally dead in the array are seen in both alternating phase and in-phase drive images.